

General Disclaimer

One or more of the Following Statements may affect this Document

- This document has been reproduced from the best copy furnished by the organizational source. It is being released in the interest of making available as much information as possible.
- This document may contain data, which exceeds the sheet parameters. It was furnished in this condition by the organizational source and is the best copy available.
- This document may contain tone-on-tone or color graphs, charts and/or pictures, which have been reproduced in black and white.
- This document is paginated as submitted by the original source.
- Portions of this document are not fully legible due to the historical nature of some of the material. However, it is the best reproduction available from the original submission.

STUDY OF THE
TIME EVOLUTION OF THE LITHOSPHERE

Grant NAG 5-150

Final Report

For the period

1 March 1981 through 31 March 1983



Principal Investigator

Dr. Micheline C. Roufousse

Prepared for
National Aeronautics and Space Administration
Goddard Space Flight Center
Greenbelt, Maryland 20771

May 1983

Smithsonian Institution
Astrophysical Observatory
Cambridge, Massachusetts 02138

The Smithsonian Astrophysical Observatory
is a member of the
Harvard-Smithsonian Center for Astrophysics

(NASA-CR-170337) STUDY OF THE TIME
EVOLUTION OF THE LITHOSPHERE Final Report,
1 Mar. 1981 - 31 Mar. 1983 (Smithsonian
Astrophysical Observatory) 22 p
HC A02/MF A01

N83-25238

CSCI 08G G3/46

Unclas
C3654

**STUDY OF THE
TIME EVOLUTION OF THE LITHOSPHERE**

Grant NAG 5-150

Final Report

For the period

1 March 1981 through 31 March 1983

Principal Investigator

Dr. Micheline C. Roufousse

**Prepared for
National Aeronautics and Space Administration
Goddard Space Flight Center
Greenbelt, Maryland 20771**

May 1983

**Smithsonian Institution
Astrophysical Observatory
Cambridge, Massachusetts 02138**

**The Smithsonian Astrophysical Observatory
is a member of the
Harvard-Smithsonian Center for Astrophysics**

I. Introduction

Under this research grant, we studied the behavior and mechanical properties of the lithosphere. This is a prerequisite to an understanding of the mechanisms and processes that occur in the earth's mantle, which are masked by the lithosphere. For this study, we used geoid heights derived from the GEOS-3 and SEASAT radar altimeters. The study of the correlation between bathymetry and geoid heights gives information on the mechanical properties of the lithosphere, such as its thickness, which is related to the age of the lithospheric plate. By probing in several locations spanning various temporal situations, we are able to retrace the time evolution of the lithospheric plates.

We also believe that a systematic study of this type will lead to one of the following predictive capabilities: location of unknown seamounts from the knowledge of the geoid heights, prediction of gravity field from the knowledge of the topography and past history of the relief, or insight into the history of a region from the knowledge of both topography and geoid heights. To achieve this aim, several seamount chains, islands and ridges must be investigated. Several geographical areas have already been studied, including the Walvis Ridge and Rio Grande Rise in the Southern Atlantic Ocean and several seamount chains in the Central Pacific Ocean. The present study indicates that two main factors influence geoid height: conditions of creation and age of the lithosphere at the time of loading.

II. Method

In this project, we restricted ourselves to the study of linear bathymetric features, i.e., seamount chains. In studying such features, it is legitimate to consider individual satellite passes crossing the chain of seamounts at an angle as close as possible to 90 degrees. It is therefore unnecessary to go through the tedious procedure of adjusting all satellite passes into a coherent network by calculating and removing a bias and trend. Furthermore, dealing with individual satellite passes is ideal for studying the evolution along a seamount chain.

To account for the geoid signals observed so far, two models were developed: the thin-elastic-plate model and the Airy model. The thin-elastic-plate model applies when a load has been developed on a thin plate of finite thickness which is subsequently deformed. The magnitude and wavelength of the deformed area depend mostly on the flexural rigidity, which is itself proportional to the cube of the lithospheric thickness. The Airy-type model applies when the load was created simultaneously with the lithosphere (or on zero thickness lithosphere) and developed light roots in order to establish local or regional isostatic equilibrium. The methodology has been described in previous reports and will be summarized here.

The first step in our procedure is to calculate theoretical filters in wavenumber space using variable parameters for both models (for example, see Figure 1). We then Fourier-transformed these functions in normal space. Next, the bathymetry was reconstructed as rigorously as possible along the subsatellite position using available contour charts (the Uchupi charts were used in the Atlantic Ocean). Lastly, the filters were convolved with the bathymetry in order to produce a set of theoretical geoid profiles to be compared with the observed geoid heights.

III. Results

We have received the complete SEASAT Geophysical data set and we have completed its editing and organization.

Several criteria have been used to edit the data: all data points of geoid heights larger than ± 150 m have been rejected as well as all geoid heights which differed by more than 15 m from the 3 preceding and 3 following points. Furthermore, several passes have been chosen at random and the observed and calculated geoids have been plotted (see Figures 2 and 3) to check the efficacy of the rejection criteria and to strengthen them if necessary. So far, the data have proven to be of excellent quality except at the borderline between continents and oceans.

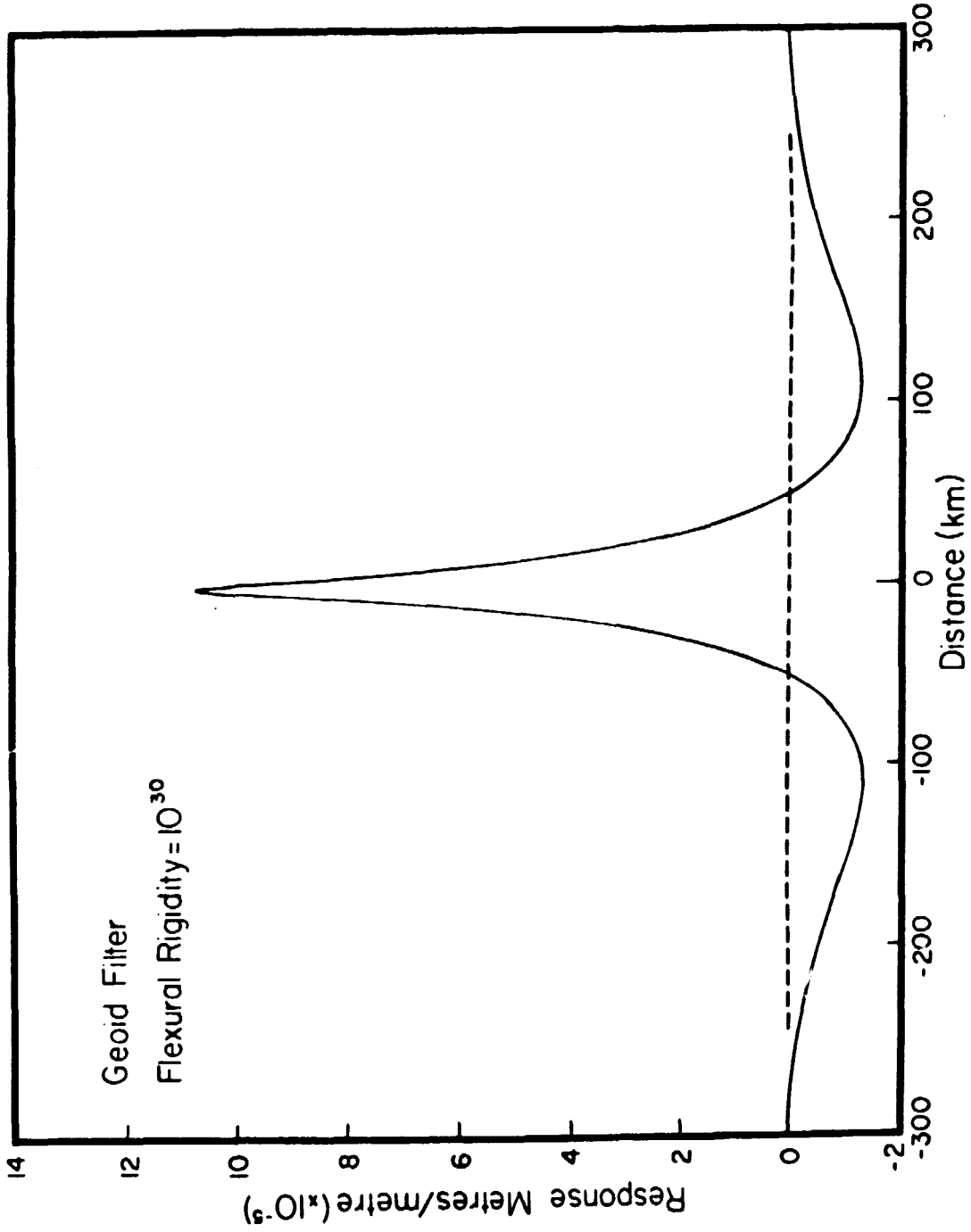


Figure 1. Geoid filter calculated by using a thin-elastic-plate model and a flexural-rigidity value of 10^{30} dyne-cm.

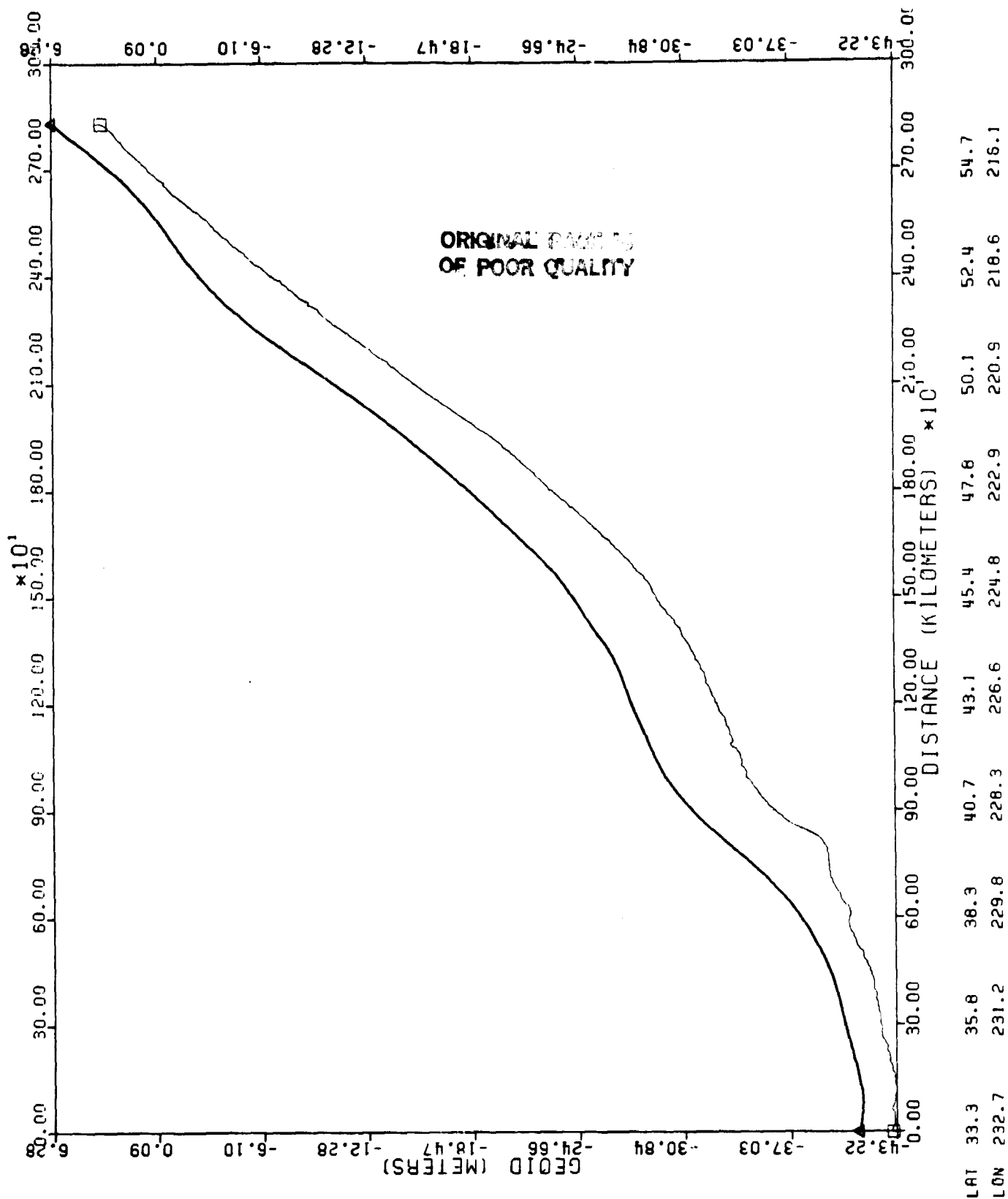
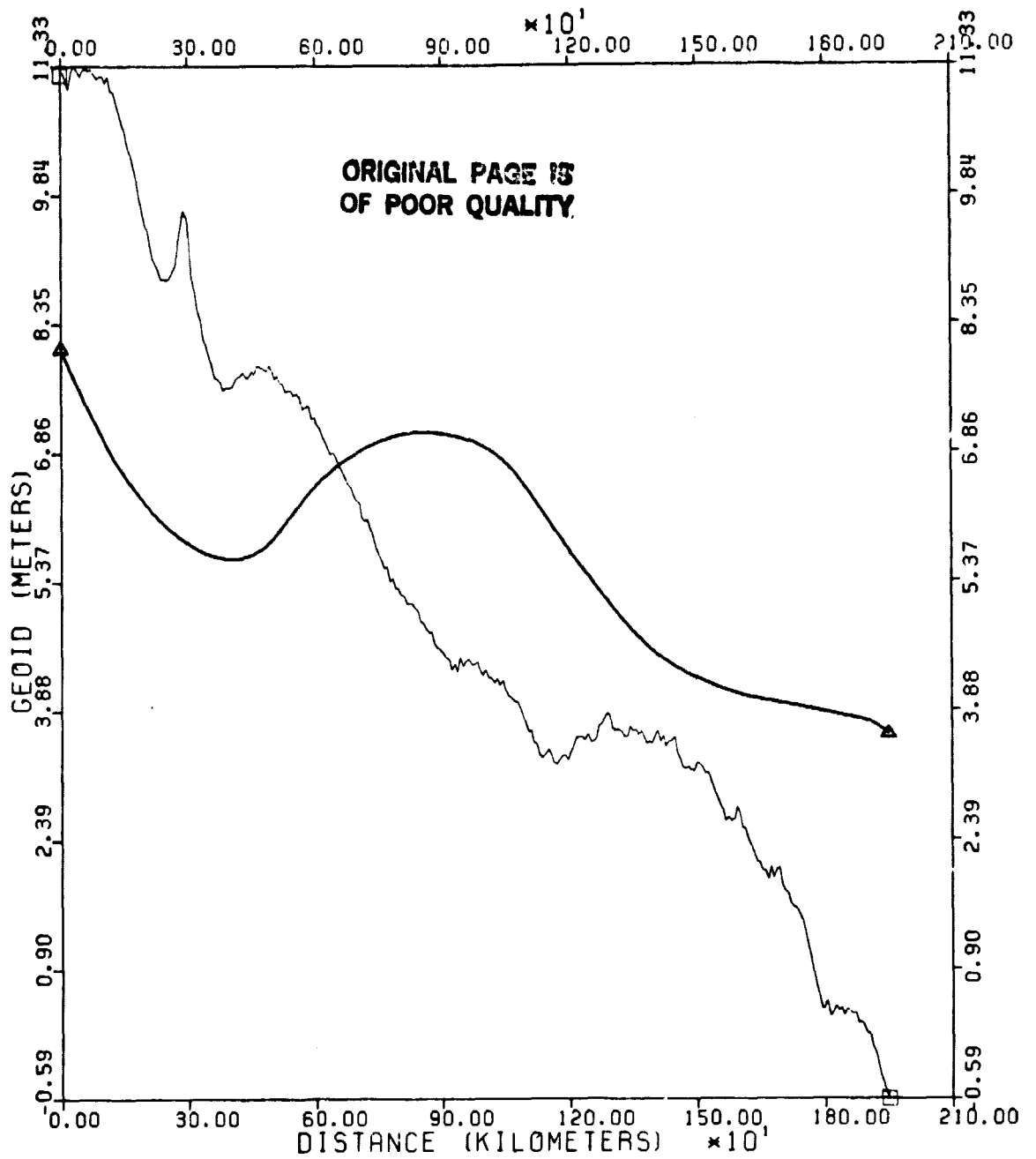


Figure 2. Observed and calculated geoid heights using SEASAT data, reduction number 954.



LAT	-31.0	-33.5	-35.9	-38.4	-40.8	-43.2	-45.5
LON	284.3	282.9	281.6	280.1	278.6	276.9	275.1

Figure 3. Observed and calculated geoid heights using SEASAT data, reduction number 1016.

In order to obtain data files of manageable size we have divided the oceans of the world into 7 regions as follows:

North Atlantic Ocean

South Atlantic Ocean

Indian Ocean

North Pacific Ocean I and II

South Pacific Ocean I and II

Each satellite pass has been divided into these 7 regions. Within each region, all the files are organized by increasing revolution number and for each file, we provide the following information: latitude, longitude, standard deviation, observed geoid, reference geoid (up to degree and order 10), residual geoid and the position along pass in each region. The data will thus be in a format compatible with that used for GEOS-3 and will permit simultaneous use of the data sets.

The data have not as yet been adjusted into a coherent network for bias and trend corrections, but the crossover errors observed so far are at the 60 cm level.

In this work, we have interpreted the geoid heights derived from the GEOS-3 and SEASAT radar altimeters. The research is divided into two main parts:

- Interpretation of the short wavelengths (ranging from 60 to 300 km) contained in the geoid spectrum; these can be explained in terms of lithospheric properties

- Interpretation of the intermediate wavelengths (ranging from 200 to 2000 km); these yield information on the properties of the convective flow occurring in the earth's interior.

Short Wavelength Study

The lithosphere is considered as a thin elastic plate; as it moves away from the ridge crest where it has been created, it ages, cools and thickens and thus its mechanical properties evolve as the thickness increases. We can probe these changes by studying the response of the lithosphere to different loading situations. For that purpose, we need to know the age of the lithosphere as well as the time and conditions of loading. In previous reports, I have described results obtained from the interpretation of the GEOS-3 radar altimeter data along the Hawaiian-Emperor Seamount chain, the New England Seamounts, the Walvis Ridge and other chains of Seamounts. Conversely, the time and conditions of loading can be derived for a specific event by comparison with known situations. I have used the SEASAT radar altimeter data to explain the formation of the Rio Grande Rise

which is located at the same latitude as the Walvis Ridge, on the Western side of the Mid-Atlantic Ridge. In a previous study performed over the Walvis Ridge, we have observed that the direction of that Ridge is incompatible with a fixed hot spot origin (see Figure 4). It is postulated that the Ridge has been formed in three main episodes by the same hot spot located at three different positions. The Eastern section was formed first by a hot spot located on the Mid-Atlantic Ridge. That hot spot then moved southward on the Mid-Atlantic Ridge and then caused the creation of the Central section of the Walvis Ridge. It finally moved toward its present location, Tristan da Cunha, off the Mid-Atlantic Ridge, and was responsible for the creation of the Western section of the Walvis Ridge.

We have thus encountered two different regimes of seamount formations: the first two segments were created on the Mid-Atlantic Ridge on zero age lithosphere and moved along with the plate to their present position. The last segment was created on young lithosphere. These two regimes give rise to different geoid signals as can be seen in Figures 5 and 6. The Seamounts formed on young lithosphere offer a much sharper signal than those formed on zero age lithosphere. We have used the thin elastic plate model to explain the geoid anomaly observed over the Western section of the Walvis Ridge. In order to explain the geoid anomaly observed over the Eastern and Central sections of the Walvis Ridge, we have used the Airy model of crustal thickening.

ORIGINAL PAGE IS
OF POOR QUALITY

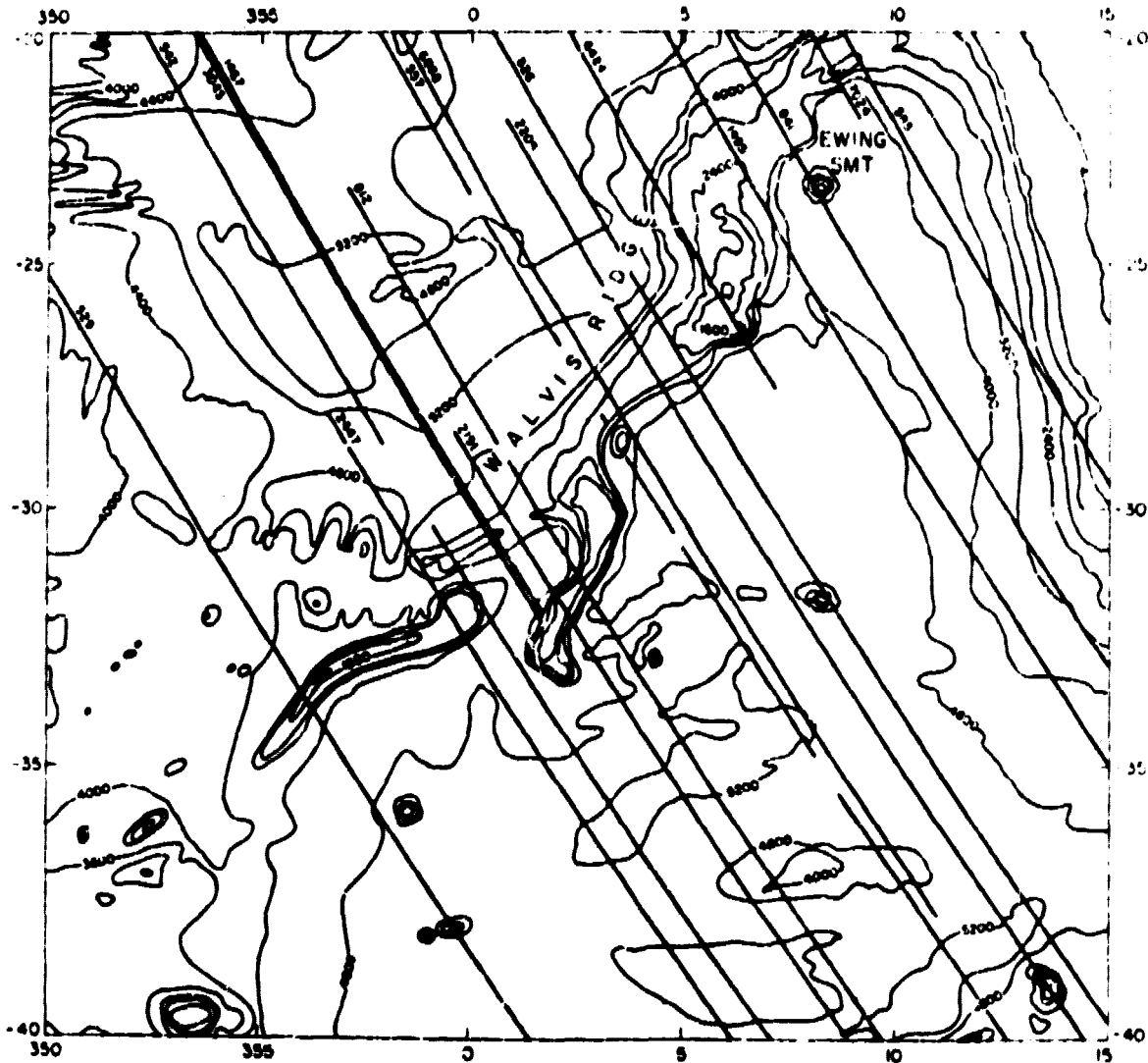


Figure 4. Bathymetry of the Walvis Ridge area and plot of the satellite passes selected over that region.

ORIGINAL PAGE IS
OF POOR QUALITY

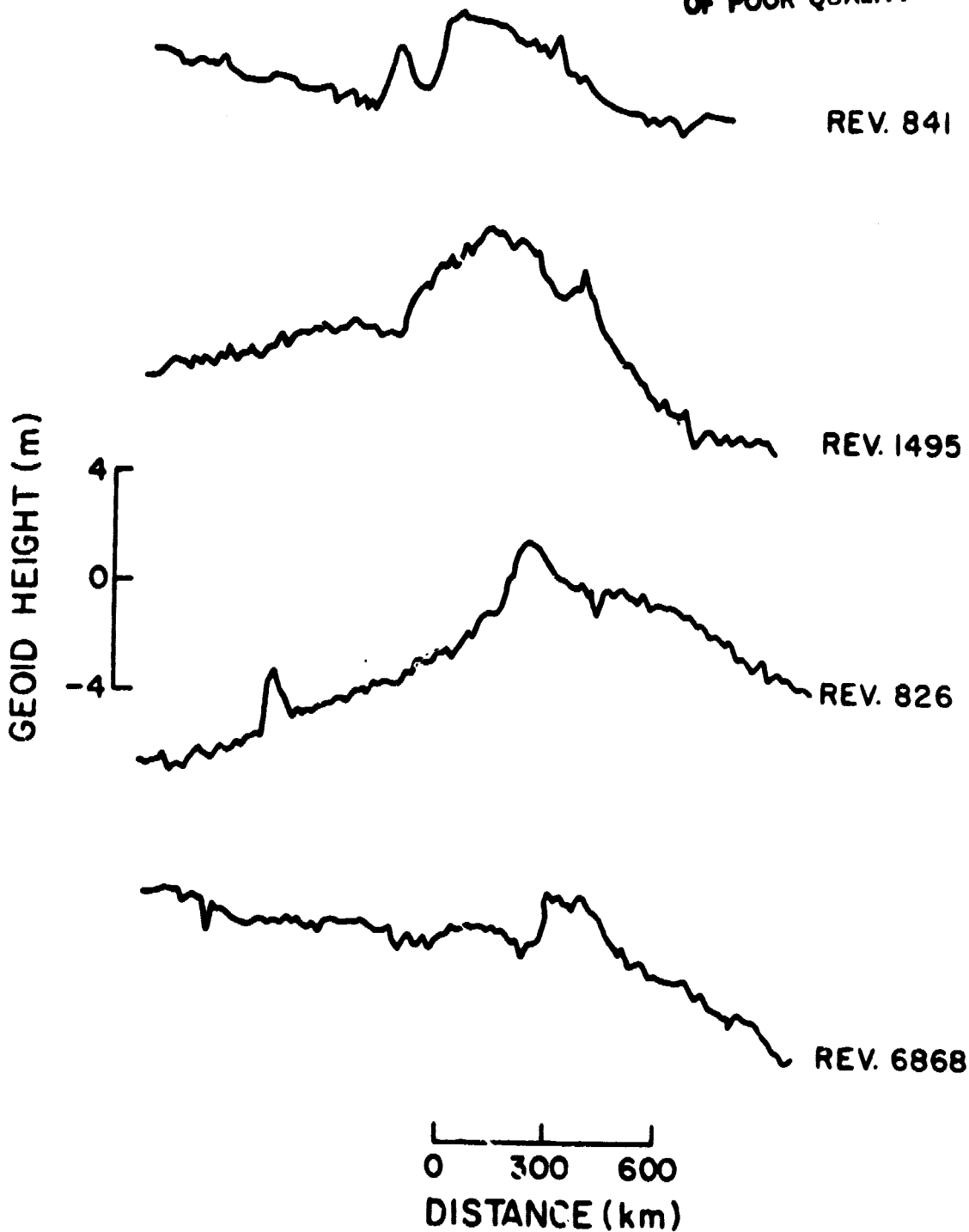


Figure 5. Four observed geoid profiles over the eastern and central sections of the Walvis Ridge represented with respect to a reference geoid of degree and order 16.

ORIGINAL PAGE IS
OF POOR QUALITY

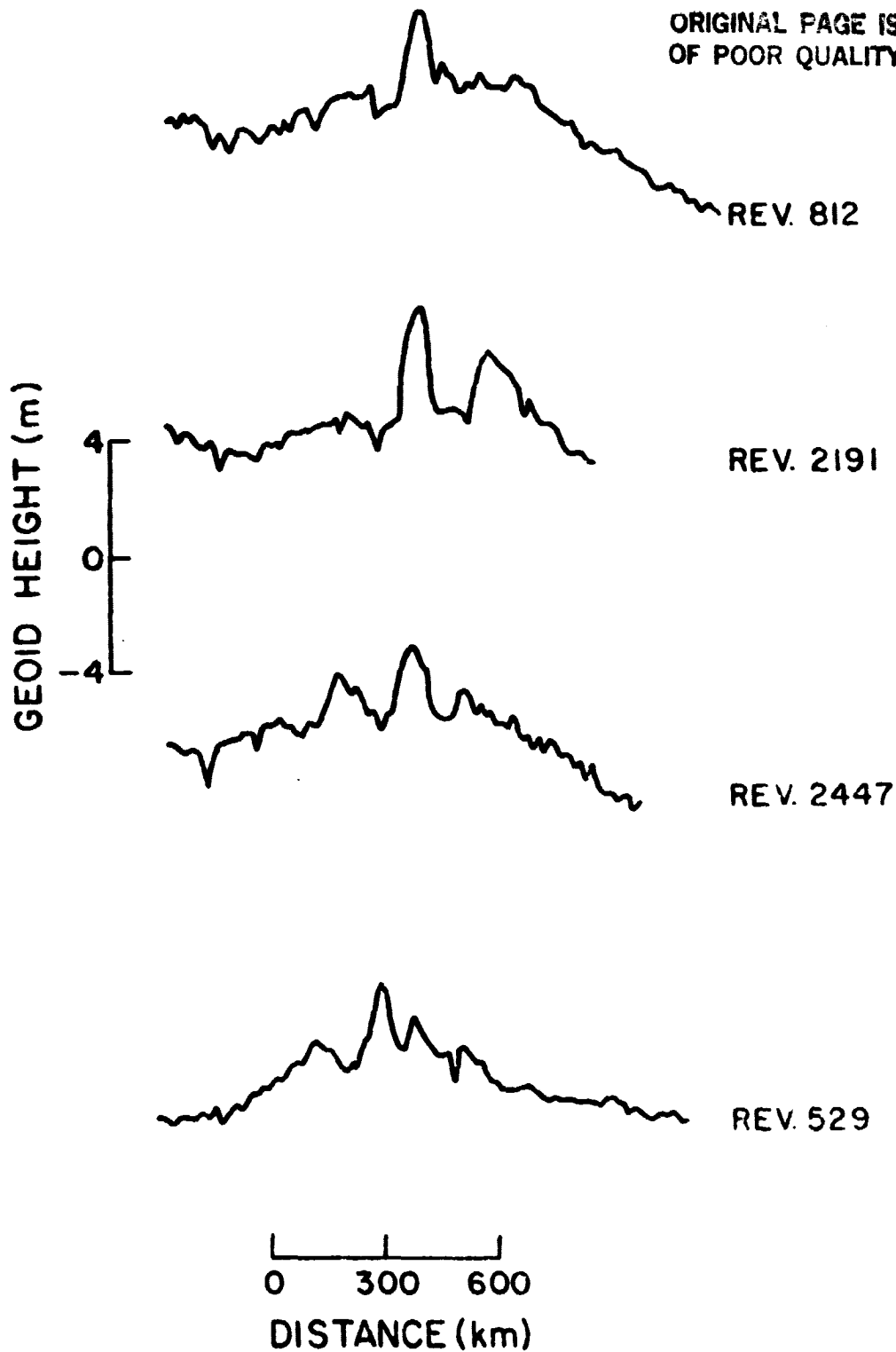


Figure 6. Four observed geoid profiles over the wester section of the Walvis Ridge, represented with respect to a reference geoid of degree and order 16.

The Rio Grande Rise developed west of the Mid-Atlantic Ridge at the same latitude as the Walvis Ridge. Figure 7 shows the SEASAT data selected for this work superposed on a sketch of the Rio Grande Rise. Figures 8 and 9 show a few satellite passes selected in that region: they all show a 4 meter deflection associated with the Ridge, superposed on a 10 to 12 meter broader geoid anomaly which can be explained only in terms of convective upwelling in the mantle. The 4 meter signal associated with the Rio Grande Rise resembles that observed across the Eastern and Central sections of the Walvis Ridge, thus suggesting a formation of the Rise, on the Mid-Atlantic Ridge, simultaneously with the Eastern and Central sections of the Walvis Ridge. A thin elastic plate model could not account for the magnitude and wavelength of the observed geoid anomaly, and we have chosen instead an Airy type model. The results obtained suggest a crustal thickening of 25 to 30 km in that region (Figure 10).

Intermediate Wavelength

The geoid heights used in this study are derived from the GEOS-3 radar altimeter. We have applied to the data the atmospheric and oceanic corrections provided with the data set. We have further corrected the data for inaccuracies in orbit determination by removing a bias and a trend provided by

ORIGINAL PAGE IS
OF POOR QUALITY

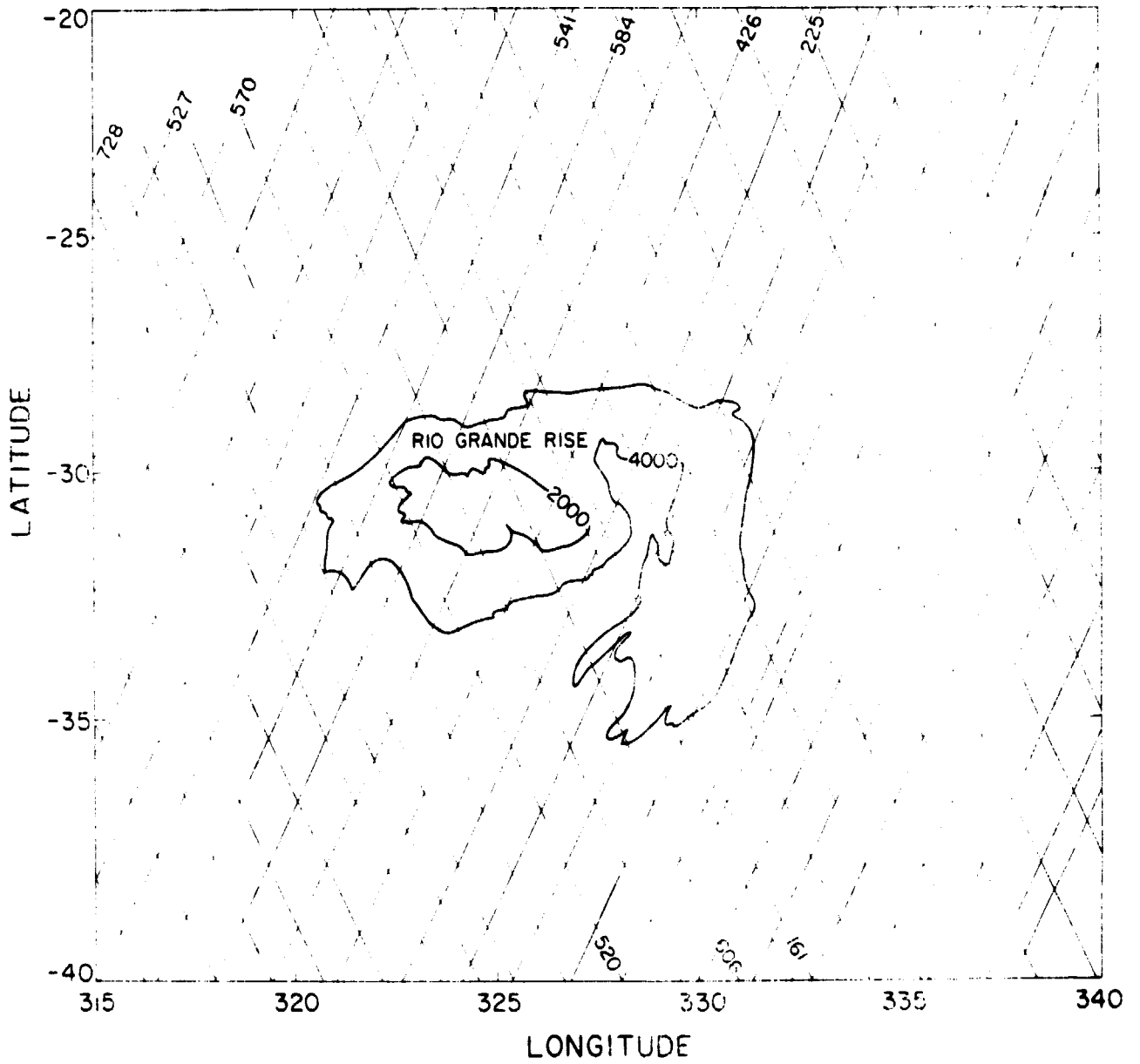


Figure 7. SEASAT radar altimeter coverage over the Rio Grande Rise

ORIGINAL PAGE IS
OF POOR QUALITY

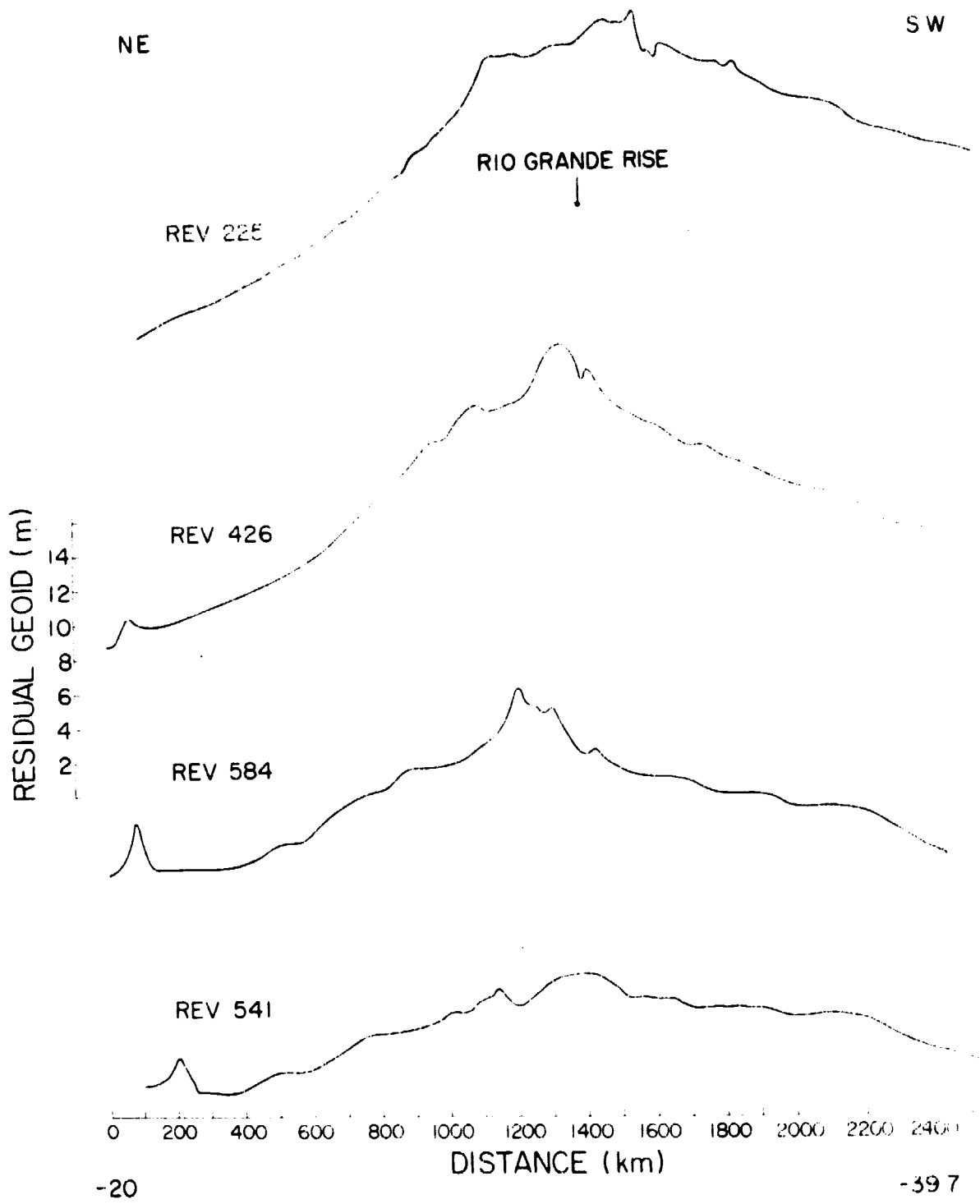


Figure 8. SEASAT radar altimeter profiles over the Grand Rise.

ORIGINAL PAGE IS
OF POOR QUALITY.

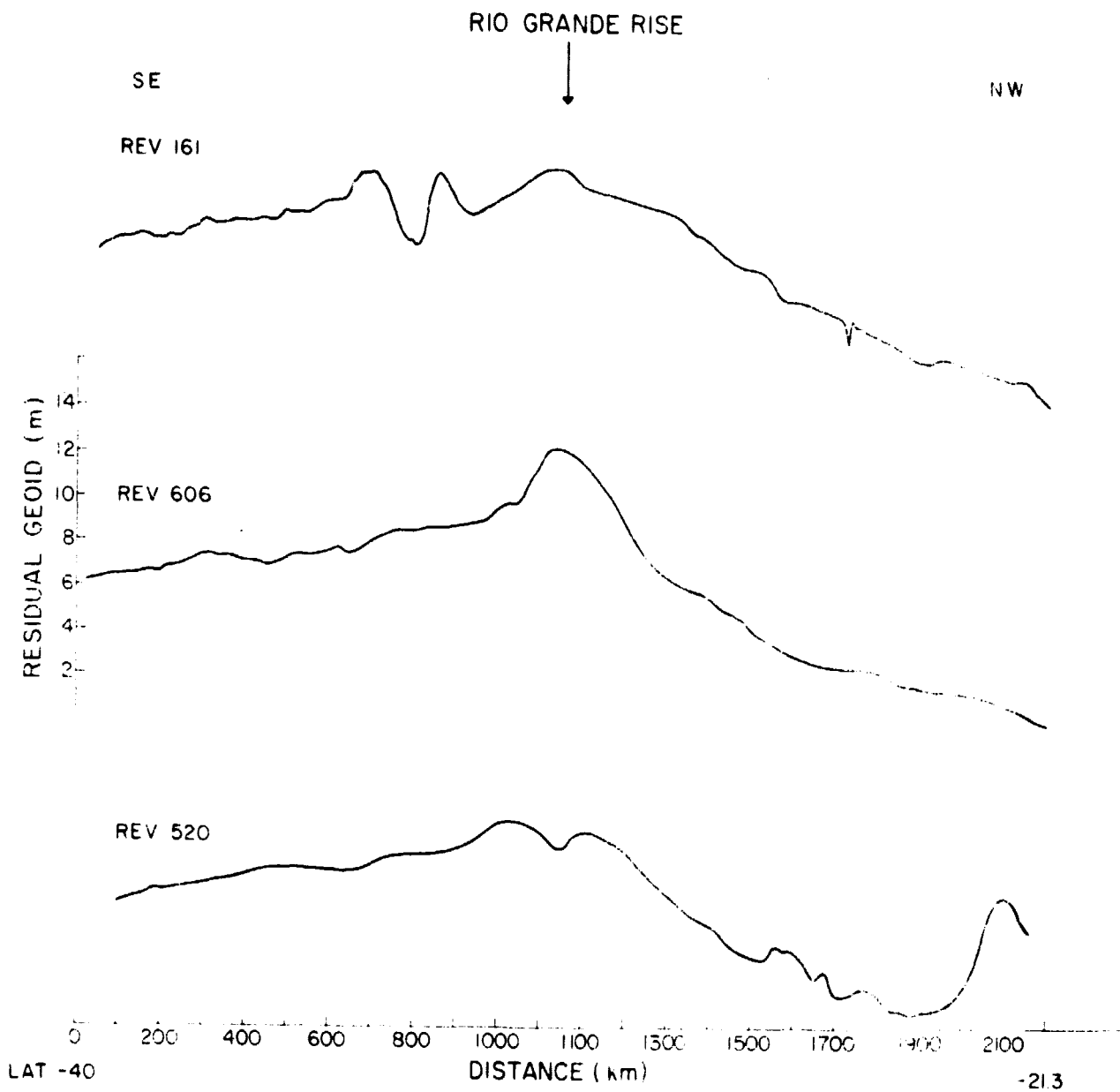


Figure 9. SEASAT radar altimeter profiles over the Rio Grand Rise.

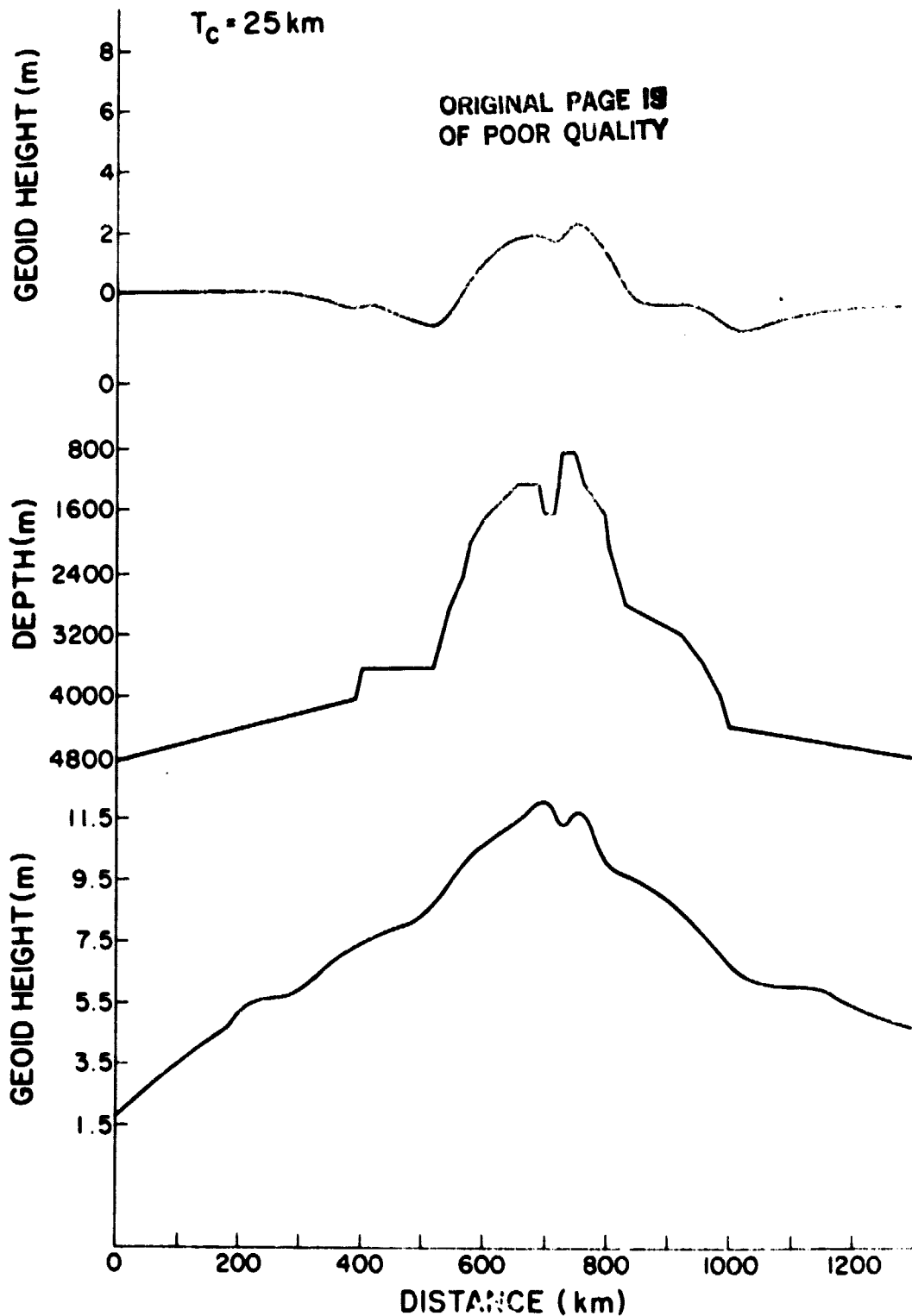


Figure 10. The bottom profile represents the observed geoid heights over the Rio Grande Rise, the intermediate profile represents the bathymetry and the top profile a theoretical geoid calculated from the Airy model with a crustal thickening of 25 km.

Dr. Rapp. We thus obtained a two-dimensional geoid of an overall accuracy of 60 cm. Because the geoid is dominated by large magnitude long wavelength anomalies, of no interest to us in this work, we have subtracted from the data a reference geoid, calculated with GEM7, up to degree and order 10. The residual geoid heights so obtained are then filtered using a Gaussian filter of half-width 100 km in order to smooth the data. These filtered values are then interpolated onto a square mesh and machine contoured. Figure 11 shows the smoothed residual geoid and Figure 12 represents the smoothed bathymetry. There is an obvious correlation between bathymetric features and geoid anomalies. These correlations fall into two categories:

1. Small geoid anomalies of the order of 2m, such as that observed over the ninety East Ridge. They can be explained totally in terms of lithospheric loading.

2. Large geoid anomalies, from 4 to 10m such as Kerguelen, South of Australia. These anomalies cannot be explained in terms of lithospheric loading; they are associated with convectively maintained density anomalies, below the lithosphere.

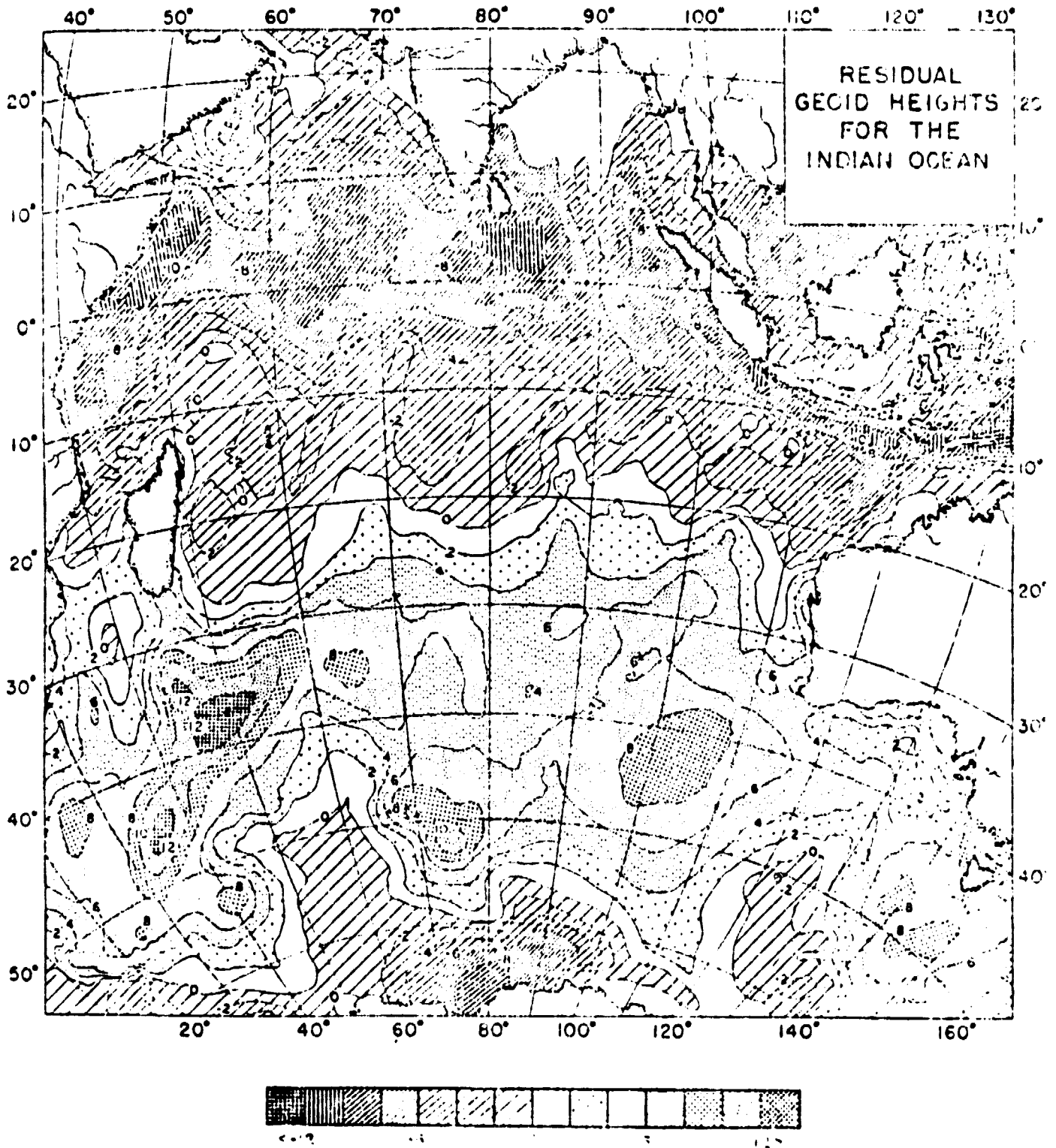


Figure 11. Residual geoid heights in the Indian Ocean.

ORIGINAL PAGE 18
OF POOR QUALITY

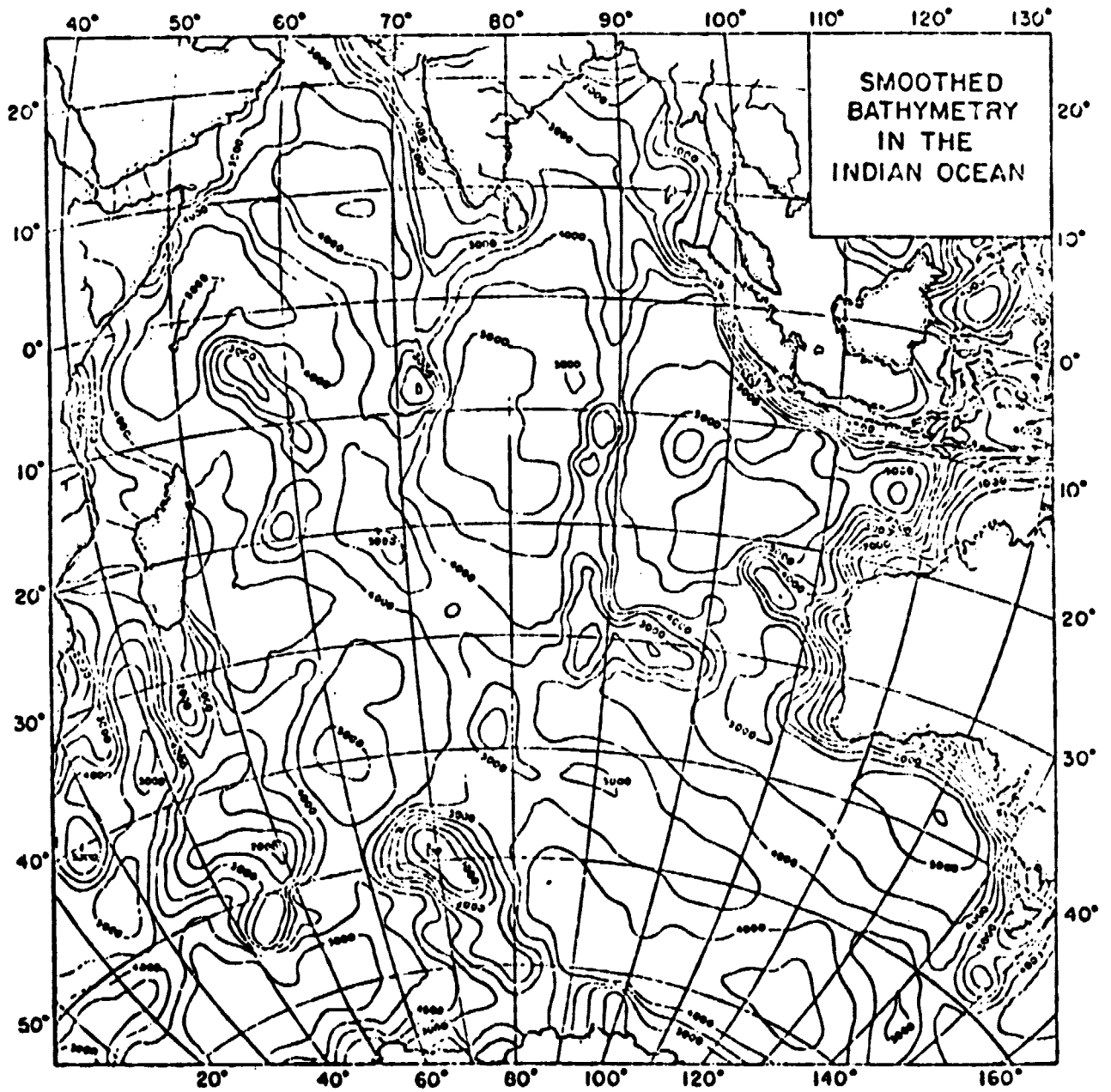


Figure 12. Smoothed bathymetry in the Indian Ocean.